# Prediction of the binding site on E1 in the assembly of the pyruvate dehydrogenase multienzyme complex of *Bacillus stearothermophilus*

Hyo-Il Jung, Richard N. Perham*

*Cambridge Centre for Molecular Recognition, Department of Biochemistry, University of Cambridge, 80 Tennis Court Road, Cambridge CB2 1GA, UK*

Received 25 September 2003; revised 24 October 2003; accepted 24 October 2003

First published online 7 November 2003

Edited by Hans Eklund

**Abstract The β-subunit (E1β) of the pyruvate decarboxylase (E1, $\alpha_2\beta_2$) component of the *Bacillus stearothermophilus* pyruvate dehydrogenase complex was comparatively modelled based on the crystal structures of the homologous 2-oxoisovalerate decarboxylase of *Pseudomonas putida* and *Homo sapiens*. Based on this homology modelling, alanine-scanning mutagenesis studies revealed that the negatively charged side chain of Glu285 and the hydrophobic side chain of Phe324 are of particular importance in the interaction with the peripheral subunit-binding domain of the dihydrolipoyl acetyltransferase component of the complex. These results help to identify the site of interaction on the E1β subunit and are consistent with thermodynamic evidence of a mixture of electrostatic and hydrophobic interactions being involved.**



*Key words:* Pyruvate dehydrogenase; Homology modelling; Multienzyme complex; Alanine-scanning mutagenesis; Protein–protein interaction

## 1. Introduction

In most organisms, the oxidative decarboxylation of pyruvate is performed by enzymes of the pyruvate dehydrogenase (PDH) complex, which consists of pyruvate decarboxylase (E1, EC 1.2.4.1), dihydrolipoyl acetyltransferase (E2, EC 2.3.1.12) and dihydrolipoyl dehydrogenase (E3, EC 1.8.1.4). Multiple copies of the three enzymes are non-covalently, but tightly, assembled into a highly organised multienzyme complex. E1 catalyses both the thiamine diphosphate-dependent decarboxylation of the pyruvate and the subsequent reductive acetylation of a lipoyl group, which is covalently bound to the E2. E2 catalyses the acyl transfer to CoA, and E3 the reoxidation of the resulting dihydrolipoyl moiety with $NAD^+$ as the ultimate electron acceptor (for reviews, see [1,2]).

E2 forms the structural core of the complex, composed of 24 or 60 E2 polypeptide chains organised with octahedral or eicosahedral symmetry, respectively, according to the source. The E2 chain has a multi-domain-and-linker structure. In the eicosahedral *Bacillus stearothermophilus* PDH complex, it consists of one lipoyl domain (LD), a peripheral subunit-binding domain (PSBD), and an acetyltransferase inner core domain (CD), which are connected by long and flexible linker segments rich in proline, alanine and charged amino acids [2,3]. The PSBD, located between the N-terminal LD and C-terminal CD, is remarkably small (only 35 amino acids) and serves to attach both E1 and E3 (mutually exclusively) to the E2 core in this as in other eicosahedral PDH complexes [2,5,6]. Analysis of the E1–E2 subcomplex by means of cryo-electron microscopy reveals the 60 E1 molecules as forming an outer shell some 90 Å above the surface of the eicosahedral inner core of 60 acetyltransferase domains [4].

The E1 component is a heterodimer ($\alpha_2\beta_2$) with molecular masses of ~41 kDa and ~36 kDa for the α- and β-chains, respectively, and the structure has been solved for the homologous E1 components of the branched-chain 2-oxo acid dehydrogenase (BCDH) complexes of *Pseudomonas putida* [7] and *Homo sapiens* [8]. A crystal structure of the *B. stearothermophilus* E3–PSBD complex has been determined [9], revealing a single PSBD bound very close to the two-fold axis of the E3 dimer, as inferred from the 1:1 stoichiometry [5,6]. No structure of the complex between the PSBD and E1 is available, but biochemical studies have again demonstrated a 1:1 stoichiometry [6] and that the E1β subunits must contain the site of association [6,10,11]. Likewise, it has been suggested that the PSBD-binding site on E1 is located at or close to the two-fold axis of the $\alpha_2\beta_2$ tetramer [6], where residues in particular from the C-terminal regions of the β-chains are located [7,8].

We show here that a plausible molecular model of the β-subunits in the E1 $\alpha_2\beta_2$ heterotetramer from the *B. stearothermophilus* PDH complex can be generated, and that this can then be used to identify amino acid residues whose side chains play an important part in the interaction with the PSBD of the E2 chain. In addition, the results throw light on the protein–protein interaction that underlies the assembly, in line with recent thermodynamic studies of the system [12–14].

## 2. Materials and methods

### 2.1. Sequence alignments and homology modelling

The amino acid sequence of the E1β chain from the *B. stearothermophilus* PDH complex (residues 1–324 out of 324) was aligned with the sequences of the E1β chains of the 2-oxoisovalerate decarboxylase

*Corresponding author. Fax: (44)-1223-333667.
*E-mail address:* r.n.perham@bioc.cam.ac.uk (R.N. Perham).

*Abbreviations:* PDH, pyruvate dehydrogenase; BCDH, branched-chain 2-oxo acid dehydrogenase; E1, pyruvate decarboxylase (EC 1.2.4.1); E2, dihydrolipoyl acetyltransferase (EC 2.3.1.12); E3, dihydrolipoyl dehydrogenase (EC 1.8.1.4); PSBD, peripheral subunit-binding domain; LD, lipoyl domain; CD, catalytic domain; ThDD, thrombin-cleavable di-domain; SPR, surface plasmon resonance

0014-5793/03/$22.00 
doi:10.1016/S0014-5793(03)01245-6

of *P. putida* (residues 3–338 out of 339) and humans (residues 19–342 out of 342). SWISS-MODEL (Automated Protein Modeling Server) was used for this purpose.

The three-dimensional structure of the E1β subunit of the *B. stearothermophilus* E1 was modelled using the program Swiss-PdbViewer (http://www.expasy.ch/spdbv/mainpage.htm) [15] connecting to Swiss Model Automated Protein Modeling Server. Modelling was based on the two crystal structures of the *P. putida* and human proteins available in the database (Protein Data Bank identification: 1QS0B and 1DTWB). The structures of the E1β subunits were superimposed and assembled to produce the E1($\beta_2$) homodimer using the graphical software MidasPlus, in which the $C_\alpha$ atoms of residues were used for the superimposition and assembly.

### 2.2. Gene manipulation and site-directed mutagenesis

A sub-gene encoding the E1β subunit in the plasmid pKBstE1b [16] was amplified by the polymerase chain reaction (PCR). The 33 bp forward primer incorporated six mismatches to create an *Xho*I restriction site at the region corresponding to 1400 bp. Primer sequences used were as follows: 5′-CCCATGCCGAACTCGAGAGTGAAACGCCGTAGC-3′ (forward, mismatches underlined) and 5′-GCTACGGCGTTTCACTCTCGAGTTCGGCATGGG-3′ (reverse). The resulting 1197 bp DNA fragment was cut with *Nco*I and *Sca*I and purified using a Qiagen Plasmid Mini-Kit (Qiagen, Chatsworth, CA, USA) after electrophoresis in a 10% polyacrylamide gel. This fragment was then ligated into *Nco*I/*Sca*I-cut, pKBstE1b expression vector. The resulting plasmid pKBstE1b(*Xho*I) was transformed into the *Escherichia coli* strain XL1 Blue. The insert DNA was completely sequenced to ensure its accuracy. This plasmid was used as a template for site-directed mutagenesis. To create E1β variants, the following primers were used: 5′ end primer: 5′-GGAATACACGATTCCGATCGGCAA-3′; 3′ end primer: 5′-GCTACGGCGTTTCACTCTCGAGTTCGGCATGGG-3′; E251A: 5′-ATCATCGGTTCGGTCGCAAAAACGGGC-3′, 5′-GCCCGTTTTTGCGACCGAACCGATGAT-3′; K252A: 5′-ATCATCGGTTCGGTCGAAGCAACGGGC-3′, 5′-GCCCGTTGCTTCGACCGAACCGATGAT-3′; R255A: 5′-GAAAAAACGGGCGCCGCCATTGTCGTT-3′, 5′-AACGACAATGGCGGCGCCCGTTTTTTC-3′; E285A: 5′-CATCTTAAGCCTTGCGGCGCCGGTGTTGCG-3′, 5′-CGCAACACCGGCGCCGCAAGGCTTAAGATG-3′; M322A: 5′-GCGAAAAAAGTGGCGAACTTCTAACAGCGGAC-3′, 5′-GTCCGCTGTTAGAAGTTCGCCACTTTTTTCGC-3′; N323A: 5′-GCGAAAAAAGTGATGGCCTTCTAACAGCGGAC-3′, 5′-GTCCGCTGTTAGAAGGCCATCACTTTTTTCGC-3′; F324A: 5′-AGTGATGAACGCCTAACAGCGGACAA-3′, 5′-TTGTCCGCTGTTAGGCGTTCATCA-3′.

For the D203A mutant, the restriction sites *Pst*I and *Xho*I were used for improved cloning efficiency. 5′ end primer: 5′-TGCGCTGCGTATCGAGTTGAAA-3′ (for the *Pst*I restriction site); 3′ end primer: 5′-GCTACGGCGTTTCACTCTCGAGTTCGGCATGGG-3′ (for the *Xho*I restriction site); D203A: 5′-AAGGAAAAGCCATCACGAT-3′, 5′-ATCGTGATGGCTTTTCCTT-3′.

### 2.3. Gene expression and protein purification

Cultures of *E. coli* strain TG1 *recO* cells transformed with plasmid pKBstE1a or pKBstE1b(*Xho*I) were grown in LB medium and induced with isopropyl-β-D-thiogalactose, and the recombinant E1($\alpha_2\beta_2$) protein was purified as described previously [16]. The purity of the protein was checked by means of sodium dodecyl sulfate–polyacrylamide gel electrophoresis using the Pharmacia PhastSystem™. The mutation in each protein was confirmed by means of electrospray mass spectrometry using a Micromass Quattro-LC spectrometer.

### 2.4. Enzymatic activity of mutant E1 components

The enzymatic activity of wild-type and mutant E1 components was determined by measuring the rate of the reduction of the artificial electron acceptor 2,6-dichlorophenolindophenol (DCPIP) in the presence of pyruvate [17]. The decrease in $A_{600}$ was monitored at a temperature of 30°C.

### 2.5. Surface plasmon resonance (SPR) detection

The interaction of the PSBD with the mutant E1 was investigated by using SPR detection [18]. A di-domain (ThDD: a LD linked to its PSBD and with a thrombin cleavage site in the linker region) was purified and immobilised on the CM5 sensor chip of a Biacore 2000 instrument using the surface thiol method to react with the lipoyl group on the LD, as described elsewhere [13,18]. The immobilisation level of the ThDD was adjusted from 100 to 250 response units to minimise any potential mass transport phenomena. To obtain kinetic parameters, E1 was injected at a flow rate of 5 μl/min to interact with the sensor surface for 10 min (association phase) at five different concentrations ranging from 12.5 to 200 nM. The flow was continued for a further 10 min with E1 omitted from the buffer to obtain the dissociation phase, all as described elsewhere [13,18]. Experimental data for each mutant were collected from five runs (sensorgrams).

## 3. Results and discussion

### 3.1. Sequence alignment for the B. stearothermophilus E1β chain

The complete amino acid sequence of the *B. stearothermophilus* E1β chain (residues 1–324) was aligned with the sequences of E1β chains from *P. putida* (residues 4–339) and human (residues 19–342), whose crystal structures have been solved at


Fig. 1. Sequence alignment of *B. stearothermophilus* E1β with *P. putida* and human E1β chains. Dark grey, identical residues; light grey, non-identical but structurally equivalent residues. Proposed secondary structure elements in the *B. stearothermophilus* E1β structure are indicated (*h*, α-helix; *s*, β-strand). BsE1β, *B. stearothermophilus* E1β; PpE1β, *P. putida* E1β; HsE1β, human E1β.

resolutions of 2.4 Å [7] and 2.7 Å [8], respectively. As depicted in Fig. 1, the *B. stearothermophilus* and *P. putida* chains show 44.7% sequence identity, and the *B. stearothermophilus* and *H. sapiens* chains exhibit 45.8% sequence identity. The alignment suggests that the *B. stearothermophilus* E1β monomer contains 11 α-helices and 14 β-strands.

### 3.2. *Homology modelling of the* B. stearothermophilus *E1β monomer*

The eicosahedral PDH complex of *B. stearothermophilus* and the octahedral BCDH complexes of *P. putida* and *H. sapiens* have a heterotetrameric ($\alpha_2\beta_2$) E1 component. To create a homology model for the *B. stearothermophilus* E1β,

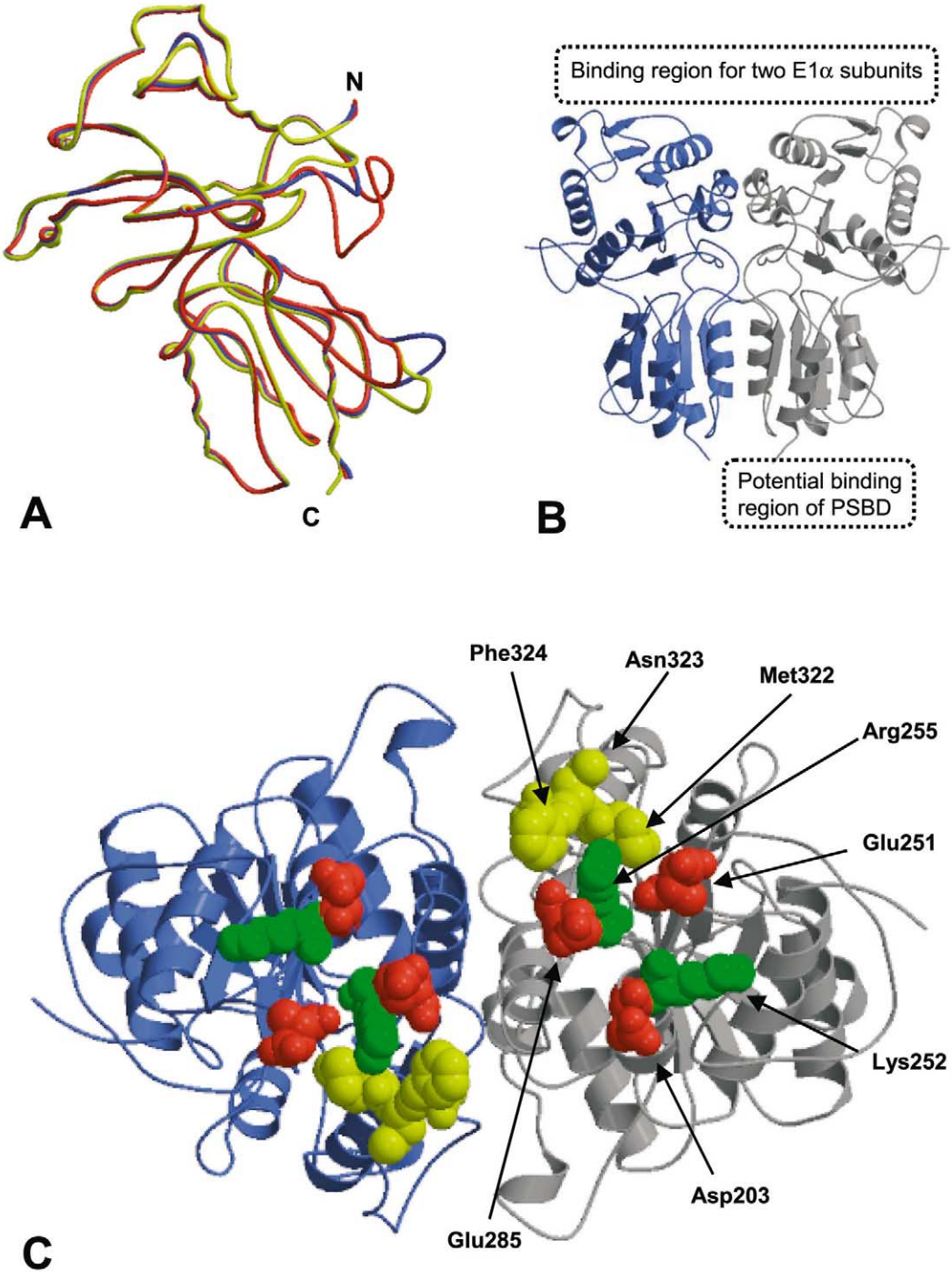


Fig. 2. Molscript [23] representation of homology-modelled structures of *B. stearothermophilus* E1β monomer and dimer. A: $C_\alpha$ trace of the predicted *B. stearothermophilus* E1β monomer (blue) superimposed on the crystallographically determined structures of *P. putida* [7] (red) and human [8] (yellow) E1β monomers. B: Dimer of the E1β subunit constructed by the program MidasPlus. One subunit is depicted in blue and the other in grey. C: Amino acid residues targeted for alanine-scanning mutagenesis in the *B. stearothermophilus* E1β dimer. The view looks up the two-fold axis of the dimer, orthogonal to the view in B. Basic residues are coloured green, acidic residues red and uncharged residues yellow. E1 is a tetramer ($\alpha_2\beta_2$) and the α-subunits have been omitted here for convenience and clarity. The α-subunits are thought not to interact with the PSBD [6]. (For interpretation of the references to color in this figure legend, the reader is referred to the web version of this article.)

we used the other two proteins as templates. A protein whose sequence has at least 40% identity to a known template structure can be modelled automatically with an accuracy approaching that of a low resolution X-ray structure or a medium resolution nuclear magnetic resonance structure [19,20]. The structure of the E1β monomer was modelled by the program SWISS-MODEL (Fig. 2A) and the dimer was constructed by graphical software MidasPlus (Fig. 2B). The backbone of the model for *B. stearothermophilus* E1β was closely superimposable on those of the templates, except for the loop regions (Fig. 2A). As in the sequence alignments (Fig. 1), the loop regions of the model structure differ from the two crystallographically determined structures at loop 15 (residues 178–195) and loop 19 (residues 237–246). However, these variable regions are highly solvent-exposed and located far from the two-fold axis of the dimer, which is expected to be at or close to the potential binding site for the PSBD of E2. Therefore, these loop regions are unlikely to play a significant part in the binding.

The E1β model structure was further analysed by using the validation software PROCHECK [21] to evaluate its stereochemical quality. A Ramachandran plot (data not shown) exhibited a good distribution for the $\phi/\psi$ angles, consistent with a good quality model. For the E1β monomer, 82.5% of (non-Gly and non-Pro) residues were in the most favoured regions, 15.6% in the additionally allowed regions, 1.1% in the generously allowed regions, and only 0.7% in the disallowed regions.

### 3.3. Identification of the residues in the E1β subunit involved in binding the PSBD of E2

The positively charged residue Arg135 and the non-polar residue Met131 of the PSBD appear to be prominently involved in binding E1 to the E2 chain of the *B. stearothermophilus* PDH complex [14]. We therefore searched for negatively charged residues, which might interact with Arg135 and non-polar residues, which might interact with Met131, among the surface residues on the E1β dimer. The binding site for PSBD on E1 is likely to be in the E1β chains in the vicinity of the E1 two-fold axis, where the C-terminal regions of the E1β chain comprise much of the surface [6–8,10,11]. In the light of the structure in Fig. 2, two residues with acidic side chains (Glu251 and Glu285) and one residue with a non-polar side chain (the C-terminal Phe324) were initially chosen for replacement with alanine. Other surface residues (Asp203, Lys252, Arg255, Met322 and Asn323) in the immediate vicinity (within 10 Å) of the centre of Glu285 were subsequently replaced with alanine to check their involvement (Fig. 2C).

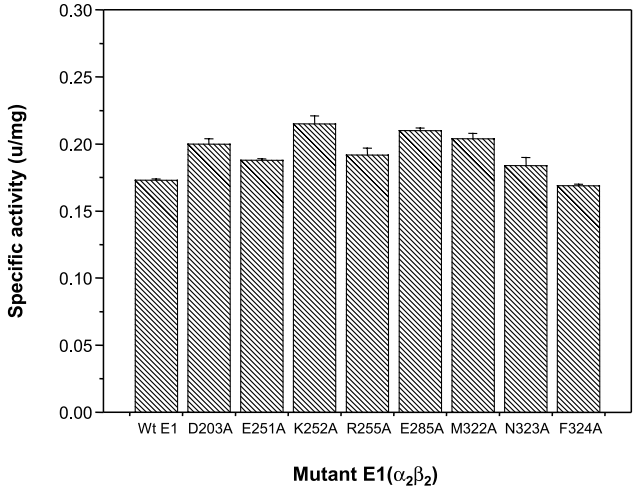


Fig. 3. Enzymatic activity of the wild-type and mutant forms of E1. The specific activities of wild-type E1 and E1 reassembled with mutant E1β chains were determined by means of the DCPIP assay [17]. Decrease in $A_{600}$ was monitored at 30°C.

The effect of the mutations in E1β on the catalytic activity of the reassembled E1 ($\alpha_2\beta_2$) tetramer was assessed using the DCPIP reduction assay. The specific activities of almost all the mutants were found to be roughly the same, if anything a little higher than that of wild-type E1 (Fig. 3). In order to test the binding affinity of E1 mutants for the wild-type PSBD, non-denaturing polyacrylamide gel electrophoresis was carried out after mixing the PSBD with the reassembled E1 ($\alpha_2\beta_2$) heterotetramer [6,13]. All the E1 mutants retained their normal capacity to bind the PSBD under these conditions (data not shown). Thus, the mutations in the E1β chain appear to be benign in terms of the overall enzymatic activity and the folding and assembly of the E1 tetramer, consistent with the fact that sites of mutation on E1β are located far from the active site of E1 ($\alpha_2\beta_2$).

SPR analysis was used to measure equilibrium dissociation constants ($K_d$) for the interaction of the mutant E1 ($\alpha_2\beta_2$) tetramers with wild-type PSBD. SPR analysis for E1 mutants E251A, E285A and F324A was performed first, followed by the other mutants: D203A, K252, R255A, M322A and N323A. For every mutant, wild-type E1 was passed through the flow cell and used as an internal reference. The kinetic

Table 1
Kinetic and thermodynamic parameters for the interaction of PSBD mutants with E1 mutants

| Proteins | | $k_{on}$(mut)/$k_{on}$(wt) | $k_{off}$(mut)/$k_{off}$(wt) | $K_d$(mut)/$K_d$(wt) | $\Delta G$ (kcal/mol)[a] |
|---|---|---|---|---|---|
| PSBD | E1 | | | | |
| WT | D203A | 1.0 | 1.5 | 1.5 | −12.7 |
| WT | E251A | 1.0 | 2.4 | 2.4 | −12.4 |
| WT | K252A | 1.0 | 1.0 | 1.0 | −12.9 |
| WT | R255A | 1.0 | 3.7 | 3.7 | −12.1 |
| WT | E285A | 1.0 | 8.6 | 8.6 | −11.6 |
| WT | M22A | 1.0 | 3.0 | 3.0 | −12.2 |
| WT | N323A | 1.0 | 2.2 | 2.2 | −12.4 |
| WT | F324A | 1.0 | 12.6 | 12.6 | −11.4 |

Kinetic data were determined by means of SPR analysis. The errors are less than ±5%.
All the measurements were performed in HBS buffer, pH 7.4 and at 25°C, as in Section 2.
The kinetic parameters of the interaction of the PSBD with E1 are $k_{on} = 3.27\times10^{6}$ $M^{-1}$ $s^{-1}$, $k_{off} = 1.06\times10^{-3}$ $s^{-1}$, $K_d = 3.24\times10^{-10}$ $M^{-1}$ [18].
[a]$\Delta G = -RT\ln K_d$, where $R = 1.987$ cal/mol/K and $T = 298$ K.

parameters were then evaluated as relative ratios (the value for a mutant divided by that for the wild-type) and are listed in Table 1.

The E285A and F324A mutations in E1β gave rise to the biggest effects on the binding affinity. The E1 mutants E285A and F324A dissociated from the wild-type PSBD about nine-fold and 13-fold faster, respectively, than wild-type E1. In contrast, the other mutations displayed little effect on the binding affinity. These results invite the speculation that Glu285 and Phe324 may be involved in the interaction with PSBD and begin to outline the E1β interface in the complex with PSBD.

### 3.4. Nature of the binding sites for PSBD on E1 and E3

The electrostatic surface potential was calculated by using the computer software GRASP [22] and mapped onto the molecular surfaces of E1, E3 and PSBD (Fig. 4). The electrostatics and surface shape of the regions around the two-fold axes of both E1 and E3 were compared. As shown in Fig. 4, the surface of helix 1 of PSBD is characterised by highly exposed positively charged residues. In the crystal structure of the E3–PSBD complex [9], three of these residues, Arg135, Arg139 and Arg156, generate an 'electrostatic zipper' with the negatively charged side chains of Asp344 and Glu431 from one subunit of the E3 dimer and E3 makes a snug fit with this region of the PSBD. The importance of these three positively charged residues in the PSBD, and in particular of Arg135, has been highlighted by mutagenesis studies [13]. In contrast, for E1, three acidic residues, Asp203, Glu251, and Glu285, protrude from the surface and are evenly distributed over the likely binding site for PSBD in the C-terminal region of E1β (Fig. 4). However, only Glu285 appears to be important for the binding to PSBD (Table 1). The presence of the C-terminal residue Phe324, the hydrophobic side chain of which also projects outwards in this region, should be noted. It is conceivable that this side chain interacts with the non-polar side chain of Met131 of the PSBD, a residue of critical importance in the binding of E1 but not of E3 [14]. A role for the C-terminal carboxyl group cannot be ruled in or out at this stage.

The binding of E3 to the PSBD is entropy-driven [12,13], despite the particular importance of electrostatic interactions and the loss of configurational entropy [9]. Conversely, E1 binding to the PSBD is more enthalpy-controlled, reflecting

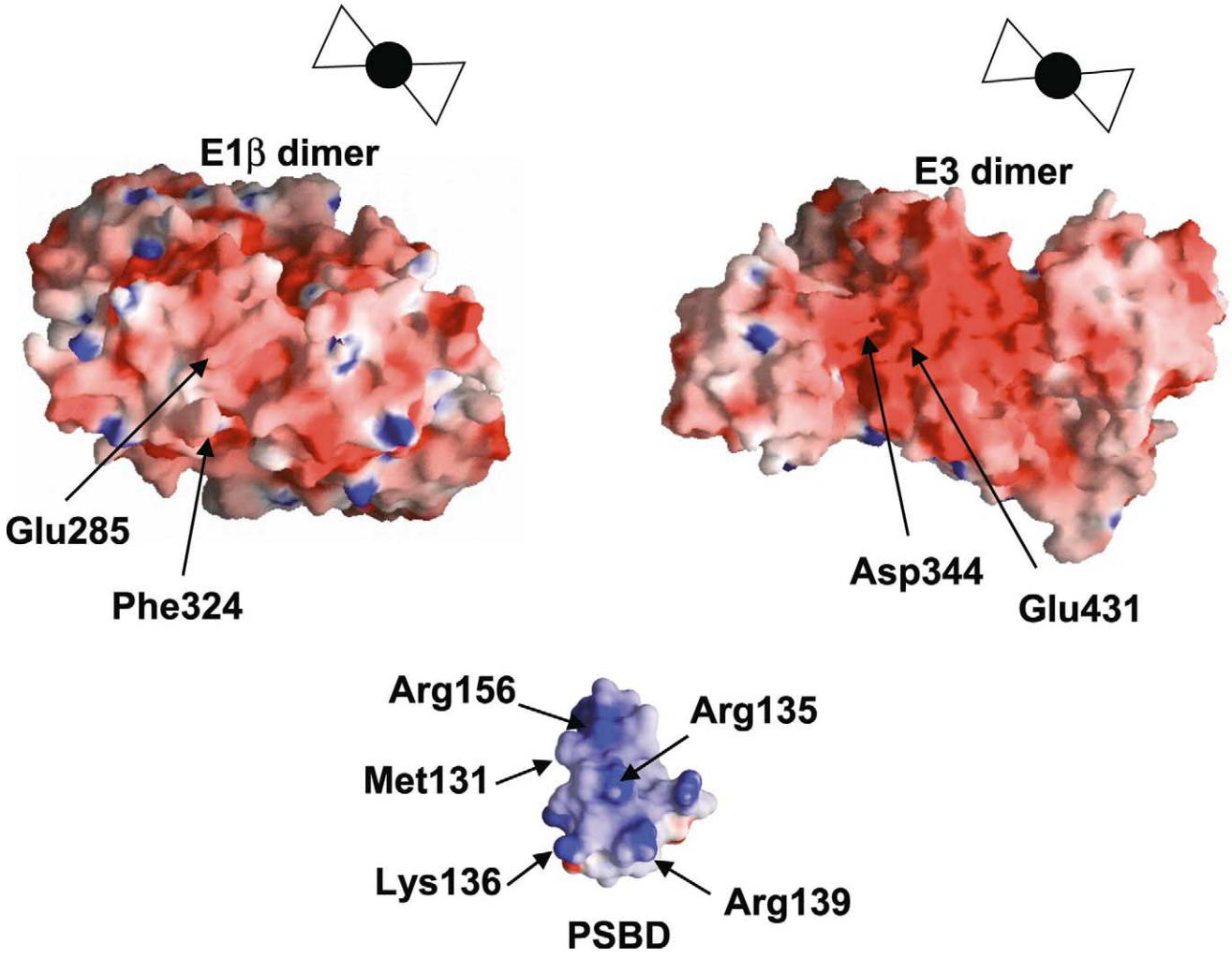


Fig. 4. Electrostatic surface potential of E1β, E3 and PSBD generated by the program GRASP [22]. Red on the surface indicates a negative potential, blue a positive potential and white a neutral potential. The electrical scale is from −14 to +9. The structures of the E1β and E3 dimers are viewed looking at the PSBD-binding sites. The closed circles indicate the direction of the two-fold axes and the two triangles represent protein monomers. Residues whose side chains are involved in binding for E1–PSBD (putative) and for E3–PSBD [9,13] are labelled. (For interpretation of the references to color in this figure legend, the reader is referred to the web version of this article.)

a more balanced mixture of hydrophobic and electrostatic interactions between E1 and PSBD [12,14]. The two different binding surfaces between E1 and PSBD, and E3 and PSBD (Fig. 4), are characterised by substantially different thermodynamic parameters but similar kinetics of interaction [12–14]. Two key residues for the E1–PSBD interaction have been identified in the present study, and a putative binding site on E1 delineated at least in part. A full interpretation of the thermodynamic parameters of the interaction must await the determination of a three-dimensional structure for the E1–PSBD complex.

*Acknowledgements:* This work was supported in part by a research grant (to R.N.P.) from the Biotechnology and Biological Sciences Research Council. We are grateful to the BBSRC and The Wellcome Trust for their support of the core facilities in the Cambridge Centre for Molecular Recognition. We thank the Cambridge Overseas Trust, the Department of Biochemistry and St John's College, Cambridge for financial support to H.I.J.

## References

[1] de Kok, A., Hengeveld, A.F., Martin, A. and Westphal, A.H. (1998) Biochim. Biophys. Acta 1385, 353–366.
[2] Perham, R.N. (2000) Annu. Rev. Biochem. 69, 961–1004.
[3] Hawkins, C.F., Borges, A. and Perham, R.N. (1990) Eur. J. Biochem. 191, 337–346.
[4] Milne, J.L.S., Shi, D., Rosenthal, P.B., Sunshine, J.S., Domingo, G.J., Wu, X., Brooks, B.R., Perham, R.N., Henderson, R. and Subramaniam, S. (2002) EMBO J. 21, 1–12.
[5] Hipps, D.S., Packman, L.C., Allen, M.D., Fuller, C., Sakaguchi, K., Appella, E. and Perham, R.N. (1994) Biochem. J. 297, 137–143.
[6] Lessard, I.A.D. and Perham, R.N. (1995) Biochem. J. 306, 727–733.
[7] Ævarsson, A., Seger, K., Turley, S., Sokatch, J.R. and Hol, W.G.J. (1999) Nat. Struct. Biol. 6, 785–792.
[8] Ævarsson, A., Chuang, J.L., Wynn, R.M., Turley, S., Chuang, D.T. and Hol, W.G.J. (1999) Structure 8, 277–291.
[9] Mande, S.S., Sarfaty, S., Allen, M.D. and Perham, R.N. (1996) Structure 4, 277–286.
[10] Wynn, R.M., Chuang, J.L., Davie, J.R., Fisher, C.W., Hale, M.A., Cox, R.P. and Chuang, D.T. (1992) J. Biol. Chem. 267, 1881–1887.
[11] Stepp, L.R. and Reed, L.J. (1985) Biochemistry 24, 7187–7191.
[12] Jung, H.I., Bowden, S.J., Cooper, A. and Perham, R.N. (2002) Protein Sci. 11, 1091–1100.
[13] Jung, H.I., Cooper, A. and Perham, R.N. (2002) Biochemistry 41, 10446–10453.
[14] Jung, H.I., Cooper, A. and Perham, R.N. (2003) Eur. J. Biochem. in press.
[15] Guex, N. and Peitsch, M.C. (1997) Electrophoresis 18, 2714–2723.
[16] Lessard, I.A.D. and Perham, R.N. (1994) J. Biol. Chem. 269, 10378–10383.
[17] Khailova, L.S., Bernkhardt, R. and Hübner, G. (1977) Biokhimiia 42, 113–117.
[18] Lessard, I.A.D., Fuller, C. and Perham, R.N. (1996) Biochemistry 35, 16863–16870.
[19] Whittle, P.J. and Blundell, T.L. (1994) Annu. Rev. Biophys. Biomol. Struct. 23, 349–375.
[20] Sanchez, R. and Sali, A. (1997) Curr. Opin. Struct. Biol. 7, 206–214.
[21] Laskowski, R.A., MacArthur, M.W., Moss, D.S. and Thornton, J.M. (1993) J. Appl. Crystallogr. 26, 283–291.
[22] Nicholls, A., Sharp, K.A. and Honig, B. (1991) Proteins 11, 281–296.
[23] Kraulis, P. (1991) J. Appl. Crystallogr. 24, 946–950.